

Plasmon reflection reveals local electronic properties of natural graphene wrinkles

Runkun Chen(陈闰堃), Cui Yang(杨翠), Yuping Jia(贾玉萍), Liwei Guo(郭丽伟), Jianing Chen(陈佳宁)
Citation: Chin. Phys. B . 2019, 28(11): 117302 . **doi:** 10.1088/1674-1056/ab46a2
Journal homepage: http://cpb.iphy.ac.cn; http://iopscience.iop.org/cpb

What follows is a list of articles you may be interested in

Review of flexible and transparent thin-film transistors based on zinc oxide and related materials

Yong-Hui Zhang(张永晖), Zeng-Xia Mei(梅增霞), Hui-Li Liang(梁会力), Xiao-Long Du(杜小龙)
Chin. Phys. B . 2017, 26(4): 047307 . **doi:** 10.1088/1674-1056/26/4/047307

Enhancement of subgap conductance in a graphene superconductor junction by valley polarization

Chuan-Xin Li(李传新), Sa-Ke Wang(汪萨克), Jun Wang(汪军)
Chin. Phys. B . 2017, 26(2): 027304 . **doi:** 10.1088/1674-1056/26/2/027304

Quantum transport through a multi-quantum-dot-pair chain side-coupled with Majorana bound states

Zhao-Tan Jiang(江兆潭), Cheng-Cheng Zhong(仲成成)
Chin. Phys. B . 2016, 25(6): 067302 . **doi:** 10.1088/1674-1056/25/6/067302

Resonant Andreev reflection in a normal-metal/quantum-dot/superconductor system with coupled Majorana bound states

Su-Xin Wang(王素新), Yu-Xian Li(李玉现), Jian-Jun Liu(刘建军)
Chin. Phys. B . 2016, 25(3): 037304 . **doi:** 10.1088/1674-1056/25/3/037304

Anomalous microwave reflection from a metal surface induced by spoof surface plasmon

Wang Liang, Cao Jin-Xiang, Lü You, Liu Lei, Du Yin-Chang, Wang Jian
Chin. Phys. B . 2012, 21(1): 017301 . **doi:** 10.1088/1674-1056/21/1/017301

RAPID COMMUNICATION

Plasmon reflection reveals local electronic properties of natural graphene wrinkles*

Runkun Chen(陈闰堃)[1], Cui Yang(杨翠)[1], Yuping Jia(贾玉萍)[2,3], Liwei Guo(郭丽伟)[4,5,6,†], and Jianing Chen(陈佳宁)[1,6,‡]

[1] *Beijing National Laboratory for Optical Physics, Institute of Physics, Chinese Academy of Sciences, University of Chinese Academy of Sciences, Beijing* 100190, *China*
[2] *Beijing National Laboratory for Condensed Matter Physics, Institute of Physics, Chinese Academy of Sciences, Beijing* 100190, *China*
[3] *Changchun Institute of Optics, Fine Mechanics and Physics, Chinese Academy of Sciences, Jilin* 130033, *China*
[4] *Research and Development Center for Functional Crystals, Laboratory of Advanced Materials and Electron Microscopy, Beijing National Laboratory for Condensed Matter Physics, Institute of Physics, Chinese Academy of Sciences, Beijing* 100190, *China*
[5] *Center of Materials Science and Optoelectronics Engineering, University of Chinese Academy of Sciences, Beijing* 100190, *China*
[6] *Songshan Lake Materials Laboratory, Dongguan* 523808, *China*

(Received 15 August 2019; revised manuscript received 12 September 2019; published online 18 October 2019)

We systematically studied surface plasmons reflection by graphene wrinkles with different heights on SiC substrate. Combined with numerical simulation, we found that the geometry corrugation of a few nanometer height wrinkle alone does not causes a reflection of graphene plasmons. Instead, the separated wrinkle from substrate exhibits a nonlinear spatial Fermi energy distribution along the wrinkle, which acts as a heterojunction. Therefor a higher graphene wrinkle induces a stronger damped region when propagating graphene surface plasmons encounter the wrinkle and get reflected.

Keywords: graphene plasmons, wrinkle, reflection, electronics

PACS: 73.20.Mf, 61.48.Gh, 72.80.Vp **DOI:** 10.1088/1674-1056/ab46a2

1. Introduction

Surface plasmon polariton, coupling between the collective oscillation of free carriers and the excitation light, is strongly confined at the metal–medium interface, which has great potential in the plasmonic devices.[1–8] Moreover, graphene has tunable carrier concentration and high carrier mobility,[9–13] which supports plasmons propagation on a two-dimensional (2D) plane in infrared regimes and draws great attention in electronics and plasmonics.[14–16] Epitaxial graphene grown on SiC substrate is widely used to obtain large area and high crystal quality graphene,[17,18] and has a great potential in electronic applications[19] and graphene-based plasmonic devices.[20–23] However, due to the compressive strain caused by the different thermal expansion coefficients of graphene and SiC in the annealing process, graphene wrinkle is widely existed on the epitaxial graphene.[24–26] The most important issue for graphene based devices is the electronic property of the wrinkle and how these wrinkles affect the graphene plasmons.

Based on the near-field optical technology, researchers observed graphene plasmons reflected by edges,[14] steps,[21] or grain boundaries[27] in the real-space by scattering scanning near-field microscopy. It is also proved[27] that the grain boundaries form electronic barriers and affect the electronic transport properties. Graphene plasmons reflection by different conductivity patterns in a flat graphene[28] and by a geometry corrugation structure[29] have been studied theoretically. However, experimental study of graphene plasmons reflected by a nanometer sized graphene structure such as wrinkle has not been reported. Herein, we characterize the graphene wrinkle with Raman spectroscopy, and then utilize the scattering scanning near field optical microscopy (s-SNOM) to study how the wrinkle affects the graphene plasmons propagation. Focusing on the near-field infrared imaging of graphene plasmons propagating along epitaxial graphene on a SiC substrate, we observe a novel interference pattern between the tip-emitted and back-reflected graphene plasmons at the natural wrinkle. Combined with the numerical simulation, we conclude that the wrinkle separated with substrate forms a heterojunction with neighbor graphene due to obvious difference in carrier concentration, which induces a strong reflection of graphene plasmons compared to the negligible reflection of the geometry corrugation. These results suggest that the graphene wrinkle has nonlinear localized electronic property with important impact on graphene integrated electronic devices. We show that it is possible to conduct an optical, touching free

*Project supported by the National Key Research and Development Program of China (Grant No. 2016YFA0203500), the National Natural Science Foundation of China (Grant No. 11874407), and Strategic Priority Research Program of Chinese Academy of Sciences (Grant No. XDB 30000000).

†Corresponding author. E-mail: lwguo@iphy.ac.cn
‡Corresponding author. E-mail: jnchen@iphy.ac.cn

© 2019 Chinese Physical Society and IOP Publishing Ltd

method to explore local electronic properties of fine structures in graphene as well as in principle other 2D materials.

2. Results and discussion

To investigate the graphene surface plasmons on the epitaxial monolayer graphene, an infrared near field imaging experiment is conducted by s-SNOM. The schematic of experiment is shown in Fig. 1(a). The atomic force microscopy (AFM) probe, with radius about 25 nm, can compensate the momentum mismatch between the incident light and the surface plasmons, then excite the surface plasmons.[14,15,21] In order to suppress the background signal in the scattering signal from the tip and samples, the pseudo-heterodyne interferometric detection scheme is used to demodulate the detected signal at a higher harmonic n ($n = 3$ in this paper), then the background is subtracted from the collected signal.[30] Finally, we obtain the topography structure and graphene plasmons imaging simultaneously when the tip scanning across the epitaxial graphene sample.

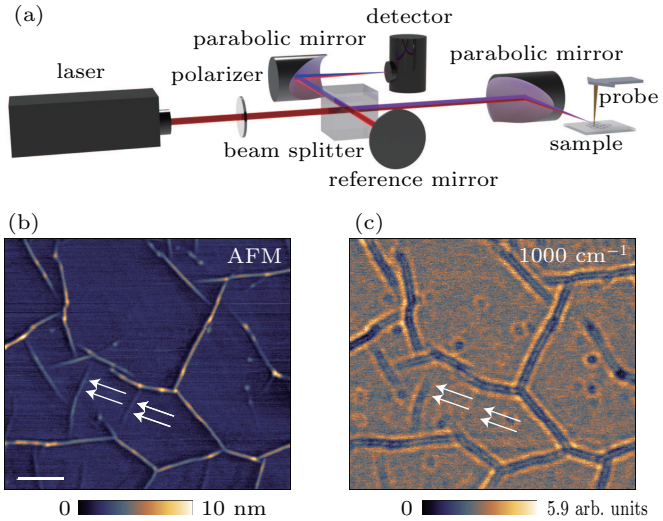


Fig. 1. Near field infrared imaging of graphene plasmons on SiC substrate. (a) The schematic diagram of s-SNOM experiment. (b) AFM topography image of graphene wrinkles on SiC substrate. (c) The corresponding infrared near field amplitude image of (b) at the frequency of 1000 cm^{-1}. The scale bar is 500 nm.

Figure 1(b) is the precise AFM topography image of the epitaxial graphene. To characterize the quality of the epitaxial graphene and the raised mesh structure in Fig. 1(b), a Raman measurement is carried. The Raman spectroscopy of the epitaxial graphene sample on SiC substrate is shown in Fig. 2. In Fig. 2(a), the Raman spectra of the bare SiC substrate (black solid line) and epitaxial graphene on SiC (blue solid line) are plotted respectively. The Raman spectrum of the pure graphene is plotted in Fig. 2(b) by subtracting the background spectrum of the SiC substrate. It seems that the epitaxial graphene is more than one layer as the intensity of the 2D peak is stronger than that of the SiC peak (1519 cm^{-1}). But we attribute it to that the focus of the laser spot is above the graphene surface, which can also be found in the previous research.[31] The ratio of I_{2D}/I_G is about 5 and the full-width half-maximum (FWHM) of the 2D band is 23.25 cm^{-1} (inset of Fig. 2(b)), which indicate that graphene grown on the SiC substrate is a monolayer graphene.[32–34] Furthermore, the absence of D band ($\sim$ 1350 cm^{-1}) means a high quality of crystal structure in the monolayer epitaxial graphene,[32,35] which suggests the raised structure in Fig. 2(b) is a continuous graphene wrinkle and no edge or crack exists. More information of the Raman mappings of the epitaxial monolayer graphene is shown in Fig. S1 of supporting information. Figure 1(c) is the optical near-field amplitude image (3th harmonics) at an incident frequency of 1000 cm^{-1} corresponding to the same region in Fig. 1(b). An obvious feature is observed that the brightest twin fringes occur outside and parallel to the wrinkle. It is consistent with the previous report[27] that graphene plasmons were reflected by the grain boundaries. In Fig. 3, we analyze a 1 μm×1 μm zoom-in area in Fig. 1(b), which has a higher resolution. The topography and near field infrared imaging are shown in Figs. 3(a) and 3(b), respectively. The topography height and normalized near field amplitude of the line profiles taken along the white dash lines in Figs. 3(a) and 3(b) are shown in Fig. 3(c). It is clear that the bright fringe occurs outside the wrinkle. Furthermore, the

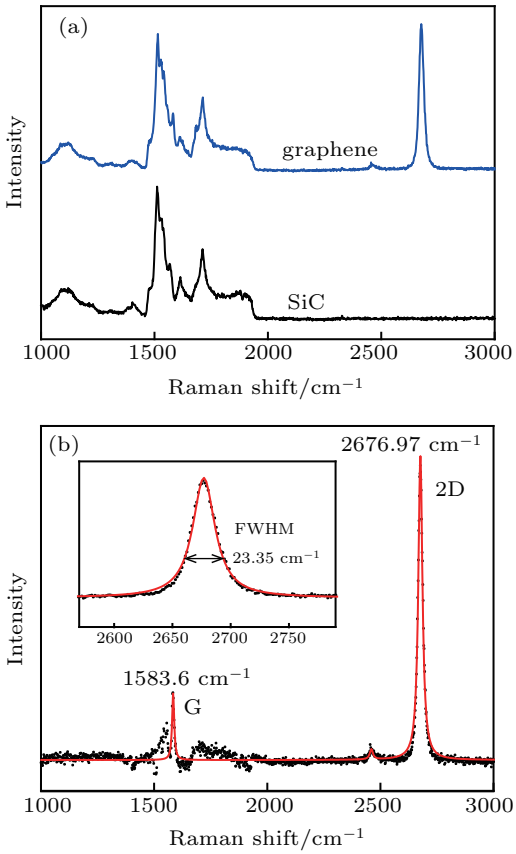


Fig. 2. The Raman spectroscopy of epitaxial monolayer graphene on SiC substrate. (a) Raman spectra of graphene and SiC substrate, respectively. (b) Raman spectrum of monolayer graphene on SiC after subtracting the SiC background. The inset is Lorentz fitting of the 2D band.

fringe width also changes with the incident light. Here we compare the theoretical graphene plasmons wavelength on SiC substrate and the fringe width in Fig. 3(d). The black square is two times of fringe width extracted from the experiments and the blue curve represents the theoretical relation of graphene plasmons on SiC substrate. It is noteworthy that the fringe width is in good agreement with the theoretical dispersion of graphene plasmons, which certifies that the fringe is the interference of the tip-emitted and back-reflected plasmons by the wrinkle.[14,15,27]

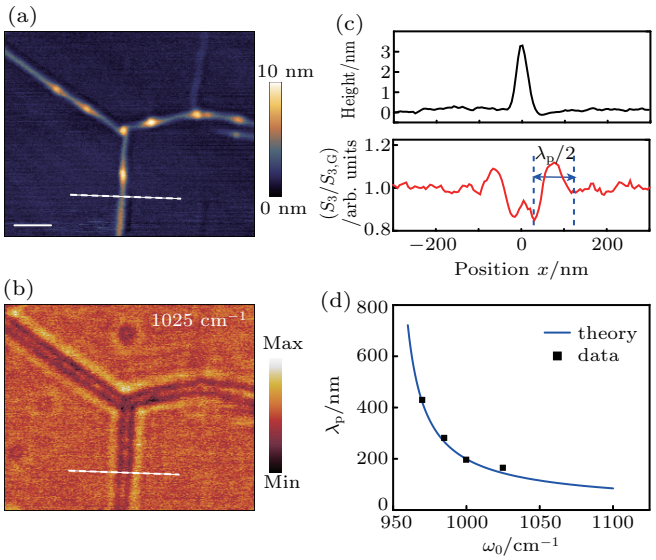


Fig. 3. The dispersion of graphene plasmons on SiC substrate. (a) Topography image of a 1 μm×1 μm area in Fig. 1(b). (b) The infrared near field imaging of (a) at the frequency of 1025 cm^{-1}. (c) Topography height (upper) and normalized near field amplitude (lower) of the line profiles taken along the white dash lines in (a) and (b). (d) Relationship of graphene plasmons wavelength and incident frequency. The blue curve and black square represent the theoretical result and experimental data, respectively. The scale bar is 200 nm.

There is also an important feature that the amplitude of fringes is related with the height of graphene wrinkles in Figs. 1(b) and 1(c). As shown in Fig. 1(b), most of wrinkle heights on the epitaxial graphene are about 3 nm, and only a few wrinkles are lower than 1 nm. The higher wrinkles show obviously interference fringes in Fig. 1(c). However, the wrinkles with lower height as indicated by the white arrows in Fig. 1(b) exhibit very weak or no fringes as shown in Fig. 1(c). The fringes amplitude profiles around different height wrinkles are shown in supporting information. It appears that the graphene plasmons reflection increases with the height of the wrinkle. In order to figure out how graphene plasmons are reflected by the wrinkle, we conduct a numerical simulation with the finite element method. The schematic of the simulation model is shown in Fig. 4(a). In the simulation model, the scanning metallic tip is treated as a point dipole with a vertically oriented momentum and the graphene with wrinkle is modeled as a surface current with $\boldsymbol{J} = \sigma \boldsymbol{E}$. Then the intensity of electric field, E, is recorded by a point probe under the electric dipole when the electric dipole scanning across the graphene. Shown as the grey line in Fig. 4(b), we calculate the electric field profile when the dipole scanning across the graphene wrinkle. Compared with the experiment data (black dot line), it suggests that the reflection by the topographic shape of the wrinkle is negligible and the strong reflection in the experiment should be caused by other reasons. More simulations with different heights of wrinkles are shown in supporting information.

It is reported[36] that the epitaxial graphene on SiC is doped because of the interaction with the substrate. Obviously, due to the compressive force,[24] the wrinkle is separated from the SiC substrate at the narrow region, which means a weaker interaction with the substrate and results in a low doping from SiC to graphene wrinkles. In this paper, we suppose that the Fermi energy at the wrinkle changes simultaneously with the increase height of the wrinkle for simply. Thus we assume that the Fermi level at the wrinkle is decreasing with a Gaussian shape profile $E_{\mathrm{F}}(x) = E_{\mathrm{F}}(\infty)(1 - \delta\, \mathrm{e}^{-x^2/w^2})$, where $E_{\mathrm{F}}(\infty) = 0.18$ eV is the Fermi energy far away from the wrinkle corresponding to a carrier density of $n = 2.4 \times 10^{12}$ cm^{-2} which agrees with the holes carrier concentration measured in the epitaxial monolayer graphene on SiC $(11\bar{2}0)$ substrate,[37,38] w is the width of the wrinkle determined by the height profile of the wrinkle, and δ is the variation of Fermi energy relative to that of flat graphene. By adjusting the variation $\delta = 0.8$, we fit the experiment data with the simulation result (more simulation is shown in supporting information) as the red line in Fig. 4(b), which shows a good agreement. It is clear that the plasmons reflection of the wrinkle is the cause of the variation of Fermi energy instead of the geometry corrugation. For achieving a more physical understanding and analysis of the graphene plasmons reflection by the wrinkle, we calculate the spatial distribution of $|E_z|$ around the wrinkle with and without a variation of conductivity in Figs. 4(c) and 4(d). In the case of a constant conductivity of wrinkle, the spatial electric field $|E_z|$ reveals that the plasmons propagate through the wrinkle directly with a negligible reflection. While in the case of a relatively decreased conductivity ($\delta = 0.8$), $|E_z|$ shows interference fringes on the left of the wrinkle, which also suggests a strong reflection by the wrinkle.[29]

According to dc conductivity[27] $\sigma_{\mathrm{dc}} \approx (2e^2/h)(E_{\mathrm{F}}/E_\tau)$, the decreased Fermi energy results in a reduced local dc conductivity of graphene. Therefore, the region around the wrinkle can be regarded as a heterojunction with a localized variation in electronic property. Besides, it also suggests that the localized electronic property related with Fermi energy has a relationship with the height of the wrinkle, as the different plasmons reflections shown in Fig. 1 and Fig. S2. Simulated with different variations of Fermi energy (i.e., dc conductiv-

ity) (see Fig. S5), it shows that a rapidly and sharply varied dc conductivity causes a strong plasmons reflection and a slowly and slightly varying dc conductivity causes a weak plasmons reflection. The wrinkle with a height below 1 nm has a slowly varying electronic property, which is important to the fabrication of a homogenous epitaxial graphene electronic device.

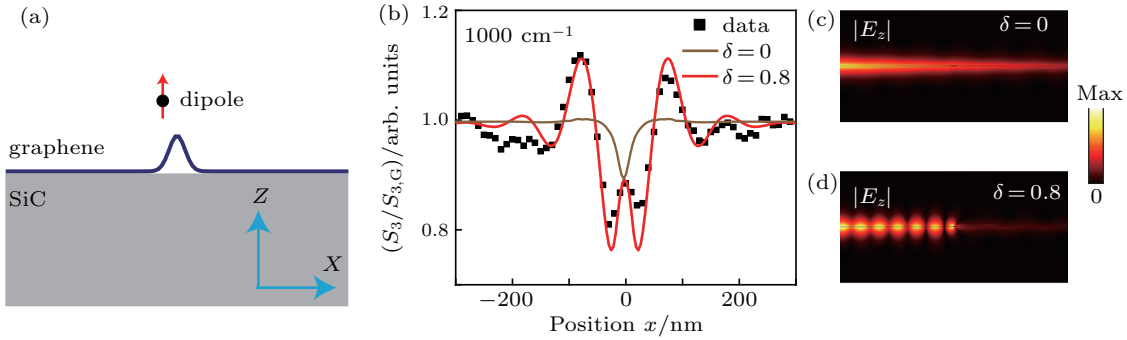


Fig. 4. The simulation of graphene plasmons reflected by the wrinkle. (a) The schematic of simulation model. (b) Comparison of experimental data (black square) and simulation results (solid line) with different variation of Fermi energy. (c) and (d) The spatial distribution of $|E_z|$ corresponding to different variation of Fermi energy.

3. Conclusion

Utilizing the scattering near-field scanning optical microscopy, we study the influence of wrinkle to the graphene plasmons. The near field imaging of graphene plasmons around the graphene wrinkles shows a novel reflection factor. Combined with the numerical simulation results, we point out that the geometry corrugation has a negligible plasmons reflection when the height of wrinkle $h \ll \lambda_p$. It is important to point out that the wrinkle separated from the substrate has a lower doping level, which means a nonlinear localized electronic property at the wrinkle. The wrinkle with a height below 1 nm has a slowly varying electronic property, which leads to a negligible reflection of graphene plasmons. While a taller wrinkle causes obvious varying of the electronic property, which gives rise to stronger plasmons reflection. This work offers a new sight to know the electronic properties of graphene wrinkle and reveals that wrinkles can be seen as a nanoscale tunable damper for further plasmonic and optoelectronic applications.

4. Method

4.1. Graphene preparation

The monolayer graphene was epitaxial growth on the nonpolar silicon carbon $(11\bar{2}0)$ by a thermal decomposition method,[39] where the graphene was raised up and separated from the substrate, then the wrinkle formed due to the different thermal expansion coefficients of graphene and SiC substrate during the cooling process.

4.2. Experiment measurements

Raman measurements The Raman spectra were measured with a Raman spectrometer with excitation laser of 532 nm. The spot size focused on the sample is about 1 μm with a 100× objective, and the power of the laser is about 1 mW. The grating spectrometer is 1800 mm^{-1}, making sure to achieve a resolution about 0.2 cm^{-1} of Raman spectra.

Near field s-SNOM measurements The near field infrared nano-image experiments were conducted by the scattering-type scanning near field optical microscopy from Neaspec GmbH. The atomic force microscopy worked with a tapping mode at frequency about 300 kHz and amplitude about 30 nm. The incident infrared light was obtained by the quantum cascade lasers, with a power of 5 mW.

4.3. Calculation of plasmons dispersion

The theoretical relation of graphene plasmons on SiC substrate is determined[27] by $\lambda_p(\omega) = \frac{\pi\sigma(\omega)}{i\omega\varepsilon_0\kappa(\omega)}$, where ε_0 is the permittivity of vacuum, $\sigma(\omega)$ is the optical conductivity of graphene, $\kappa(\omega) = [1+\varepsilon_{sub}(\omega)]/2$, and $\varepsilon_{sub}(\omega)$ is the dielectric function of the SiC substrate. For the limit of long wavelength and low frequency, the optical conductivity can be written as a Drude model[21] $\sigma(\omega) = i\frac{e^2}{\pi\hbar^2}\frac{E_F}{\omega+i\tau^{-1}}$, where τ is the relaxation time and E_F is the Fermi energy.

4.4. Numerical simulation

The near field simulation of graphene wrinkle by a point dipole model and the spatial distribution of $|E_z|$ around the wrinkle are obtained by the finite element method using the commercial software Comsol. The mesh in our model is fine enough to achieve a good convergence result. The permittivity of SiC is taken from the literature.[40]

Supporting information

The following supporting information are available: Raman mapping image of graphene sample, more details experiment, and simulation results of graphene plasmons reflected by the wrinkles.

Acknowledgement

We thank Alexey Nikitin for original simulation modeling ideas and discussions.

References

[1] Ritchie R H 1957 *Phys. Rev. D* **106** 874
[2] Barnes W L, Dereux A and Ebbesen T W 2003 *Nature* **424** 824
[3] Gramotnev D K and Bozhevolnyi S I 2010 *Nat. Photon.* **4** 83
[4] Chen W, Hu H, Jiang W, Xu Y, Zhang S and Xu H 2018 *Chin. Phys. B* **27** 107403
[5] Qurban M, Tahira R, Ge G Q and Ikram M 2019 *Chin. Phys. B* **28** 030304
[6] Lu H, Fan Y C, Dai S Q, Mao D, Xiao F J, Li P and Zhao J L 2018 *Chin. Phys. B* **27** 117302
[7] Liu C P, Zhang J S, Xu J, Wang Y L and Yu D P 2016 *Chin. Phys. Lett.* **33** 87303
[8] Cheng Z Q, Yu P and Liu Z M 2018 *Acta Phys. Sin.* **67** 197302
[9] Geim A K and Novoselov K S 2007 *Nat. Mater.* **6** 183
[10] Bolotin K I, Sikes K, Jiang Z, Klima M, Fudenberg G, Hone J, Kim P and Stormer H 2008 *Solid State Commun.* **146** 351
[11] Ju L, Geng B, Horng J, Girit C, Martin M, Hao Z, Bechtel H A, Liang X, Zettl A and Shen Y R 2011 *Nat. Nanotechnol.* **6** 630
[12] Fang Z, Thongrattanasiri S, Schlather A, Liu Z, Ma L, Wang Y, Ajayan P M, Nordlander P, Halas N J and García de Abajo F J 2013 *ACS Nano* **7** 2388
[13] Fang Z, Wang Y, Liu Z, Schlather A, Ajayan P M, Koppens F H, Nordlander P and Halas N J 2012 *ACS Nano* **6** 10222
[14] Chen J, Badioli M, Alonsogonzalez P, Thongrattanasiri S, Huth F, Osmond J, Spasenovic M, Centeno A, Pesquera A and Godignon P 2012 *Nature* **487** 77
[15] Fei Z, Rodin A S, Andreev G O, Bao W, Mcleod A S, Wagner M, Zhang L M, Zhao Z, Thiemens M H and Dominguez G 2012 *Nature* **487** 82
[16] Abajo D and Garcia F J 2014 *ACS Photon.* **1** 135
[17] Hupalo M, Conrad E and Tringides M 2009 *Phys. Rev. B* **80** 041401
[18] De Heer W A, Berger C, Ruan M, Sprinkle M, Li X, Hu Y, Zhang B, Hankinson J and Conrad E 2011 *Proc. Natl. Acad. Sci. USA* **108** 16900
[19] Novoselov K S, Geim A K, Morozov S V, Jiang D, Zhang Y, Dubonos S V, Grigorieva I V and Firsov A A 2004 *Science* **306** 666
[20] Lu J, Loh K P, Huang H, Chen W and Wee A T 2009 *Phys. Rev. B* **80** 113410
[21] Chen J, Nesterov M L, Nikitin A Y, Thongrattanasiri S, Alonsogonzalez P, Slipchenko T M, Speck F, Ostler M, Seyller T and Crassee I 2013 *Nano Lett.* **13** 6210
[22] Fang Z, Liu Z, Wang Y, Ajayan P M, Nordlander P and Halas N J 2012 *Nano Lett.* **12** 3808
[23] Fang Z, Wang Y, Schlather A E, Liu Z, Ajayan P M, García de Abajo F J, Nordlander P, Zhu X and Halas N J 2013 *Nano Lett.* **14** 299
[24] Deng S and Berry V 2016 *Mater. Today* **19** 197
[25] Bao W, Miao F, Chen Z, Zhang H, Jang W, Dames C and Lau C N 2009 *Nat. Nanotechnol.* **4** 562
[26] Zhu W, Low T, Perebeinos V, Bol A A, Zhu Y, Yan H, Tersoff J and Avouris P 2012 *Nano Lett.* **12** 3431
[27] Fei Z, Rodin A S, Gannett W, Dai S, Regan W, Wagner M, Liu M, Mcleod A S, Dominguez G and Thiemens M H 2013 *Nat. Nanotechnol.* **8** 821
[28] Garcia-Pomar J L, Nikitin A Y and Martin-Moreno L 2013 *ACS Nano* **7** 4988
[29] Slipchenko T M, Nesterov M L, Hillenbr, R, Nikitin A Y and Martín-Moreno L 2017 *ACS Photon.* **4** 3081
[30] Ocelic N, Huber A J and Hillenbr R 2006 *Appl. Phys. Lett.* **89** 101124
[31] Yang R, Huang Q, Chen X, Zhang G and Gao H J 2010 *J. Appl. Phys.* **107** 034305
[32] Ferrari A C and Basko D M 2013 *Nat. Nanotechnol.* **8** 235
[33] Malard L, Pimenta M, Dresselhaus G and Dresselhaus M 2009 *Phys. Rep.* **473** 51
[34] Graf D, Molitor F, Ensslin K, Stampfer C, Jungen A, Hierold C and Wirtz L 2007 *Nano Lett.* **7** 238
[35] Ferrari A C 2007 *Solid State Commun.* **143** 47
[36] Sidorov A N, Gaskill K, Buongiorno Nardelli M, Tedesco J L, Myers-Ward R L, Eddy Jr C R, Jayasekera T, Kim K W, Jayasingha R and Sherehiy A 2012 *J. Appl. Phys.* **111** 113706
[37] Camara N, Jouault B, Caboni A, Tiberj A, Godignon P and Camassel J 2011 *Nanosci. Nanotechnol. Lett.* **3** 49
[38] Jabakhanji B, Camara N, Caboni A, Consejo C, Jouault B, Godignon P and Camassel J 2012 *Mater. Sci. Forum* **711** 235
[39] Jia Y, Guo L, Lu W, Guo Y, Lin J, Zhu K, Chen L, Huang Q, Huang J and Li Z 2013 *Sci. Chin.-Phys. Mech. & Astron.* **56** 2386
[40] Mutschke H, Andersen A C, Clement D, Henning T and Peiter G 1999 *Astron. Astrophys.* **345** 187